Polypyrrole/oligonucleotide nano-composite: its initial growth

Y Li[1], J Jiang[1]*, X Ma[1], G Dong[1], J Wang[1], and **K-L Paul Sung[1,2]**
[1]Key Laboratory of Biorheological Science and Technology, Ministry of Education, Bioengineering College, Chongqing University, Chongqing, People's Republic of China
[2]Departments of Bioengineering and Orthopaedic Surgery, University of California, San Diego, California, USA

The manuscript was received on 19 March 2009 and was accepted after revision for publication on 27 March 2009.

DOI: 10.1243/17403499JNN143

Abstract: In this work, the initial growth process of a polypyrrole/oligonucleotide (PPy/ODN) nanocomposite electrochemically synthesized on an indium tin oxide (ITO)-coated glass surface was investigated by means of chronoamperometric measurements combined with optical microscopy and atomic force microscopy (AFM). It was found that the growth of PPy/ODN onto ITO was a three-stage process including incubation, rapid nucleation and growth, and constant nucleation and growth. The presence of ODN molecules significantly shortened the first stage. Further analysis showed that the nucleation and growth mechanism of PPy/ODN was progressive nucleation and 3D growth, which then changed to instantaneous nucleation and 3D growth before nucleus overlapping. In the third stage, the nucleation and growth mechanism of PPy/ODN was a combination of progressive nucleation and 3D growth and instantaneous nucleation and 3D growth.

Keywords: nanocomposite, polypyrrole, electropolymerization, oligonucleotide

1 INTRODUCTION

DNA is a unique biomolecule that serves not only as genetic information storage in living species but also as an emerging important building block for assembly of nanoscale materials [**1**]. The hybrid of DNA molecules with conducting polypyrrole has been explored as an attractive 'bottom-up' route to forming nanostructures, such as nanowires [**2**], nanoropes [**3**], and nanocapsules [**4**]. Furthermore, polypyrrole/oligonucleotide (PPy/ODN) composite films of various thicknesses have also been attracting attention as favourable interfaces for biosensor applications [**5**–**7**]. In the latter, PPy/ODN normally may be easily formed via electropolymerization on various conducting substrates, and species of ODNs may be directly incorporated into the PPy matrix as dopants during polymer synthesis when they are included in the polymerization solution as a sole counterion [**8**, **9**] or in the presence of another electrolyte [**10**, **11**]. For the signal transduction of an electrochemical DNA biosensor, the composition at the two interfaces (electrode side and solution side) of PPy/ODN is crucial. While research has been carried out to understand the interactions occurring on the solution side and even within the network of a PPy/ODN composite [**8**–**11**], to the best of the authors' knowledge less attention has been paid to the interface on the electrode side of PPy/ODN. Indeed, the kinetics of polypyrrole electrodeposition could be influenced by different substrates [**12**–**15**], which might result in different interface compositions. In this respect, there is reason to suppose that the influence of the interface composition on the formation of some nanostructures based on PPy/ODN is great. Therefore, in the present work, the initial electrodeposition kinetics of PPy/ODN was investigated by means of chronoamperometry, atomic force microscopy (AFM), and optical microscopy to substantiate the above hypothesis.

*Corresponding author: Key Laboratory of Biorheological Science, and Technology, Ministry of Education, Bioengineering College, Chongqing, 400044, People's Republic of China.
email: jhuan@cqu.edu.cn

2 EXPERIMENTAL METHODS

All chemicals were of analytical grade and used as received (if not otherwise stated). Pyrrole monomer was obtained from Sinopharm Chemical Reagent Co. Ltd (Shanghai, China) and distilled before use. The following oligonucleotides were purchased from Shenggong Bioengineering Ltd (Shanghai, China): primer P1 (30-mer 5′-GTC TCT ACC TGA TTA CTA TTG CAT CTT CCG-3′), primer P2 (15-mer 5′-CTC TAC CTG ATT ACT ATT GC-3′), and primer P3 (10-mer 5′-GCA ATA GTA ATC AGG-3′). Other reagents were commercially available and were all of analytical reagent grade. All of the solutions were prepared in ultrapure water with the Millipore system (18.2 MΩ).

The electropolymerization of a PPy/ODN composite was carried out by the potentiostatic method in a custom-made electrochemical cell (internal volume 100 μL) with indium tin oxide (ITO)-coated glass (which had a nominal surface resistivity of 95 Ω/sq) as a working electrode (area 0.49 cm^2), a platinum wire coil as an auxiliary electrode, and an Ag/AgCl wire as a reference electrode. The electropolymerization experiments were performed in a CHI-800 electrochemical workstation (Shanghai Chenhua Ltd, Shanghai, China). The electrolytes used for the experiments were 0.05 M pyrrole in 0.1 M NaCl solution in the presence of 1×10^{-5} M P1, P2, and P3 ODNs respectively. Inverted fluorescence microscopy (Leica DMI4000B) and AFM (CSPM 5000; Ben Yuan Ltd, Beijing, China) were used to observe the nucleation and growth mechanism of PPy/DNA on the ITO surface. For contrast, the electropolymerization of polypyrrole was also conducted without ODN.

3 RESULTS AND DISCUSSION

3.1 Electropolymerization of PPy/ODN

Figure 1 presents the chronoamperometric curves of polypyrrole electrodeposited on an ITO electrode surface in the presence of 1×10^{-5} M P1 ODN (in 0.05 M pyrrole/0.1 M NaCl solution) at different potentials within a period of 200 s. At these different polymerization potentials, the chronoamperometric curves in Fig. 1(a) show their respective current maximum I_{max}. The value of I_{max} is 750 μA at 0.65 V, and therefore little PPy/ODN composite is being formed. At 0.7 V, the current increases with time and reaches an I_{max} value of 2980 μA at 130 s. At the applied potentials of 0.8 and 0.9 V, I_{max} values of 4537 and 6327 μA can be reached respectively. When the applied potential increases to 1.0 V, there is a peak current of 8900 μA at times ranging from 35 to 40 s. Comparing these curves in Fig. 1, the I_{max} value increases with the polymerization potentials. This might be due to the fact that the number of nuclei increases as the number of active sites for polymerization increases when the potentials are raised from lower to higher values [**16**]. Moreover, the time it takes for the current to reach I_{max}, T_{max}, decreases with increase in the potentials. This behaviour can be attributed to the more rapid spread and collapse of polypyrrole nuclei at higher potentials [**16**].

Figure 1(a) shows that the nucleation and growth current curves of polypyrrole in the presence of 30-mer ODN can be divided into three stages qualitatively at the applied potentials of 0.7, 0.8, and 0.9 V. This observation is similar to the result obtained by Wang *et al.* [**15**]. It can be seen that the initial current has a slight increase for a short time (stage 1, incubation), followed by a rapid increase until it reaches a

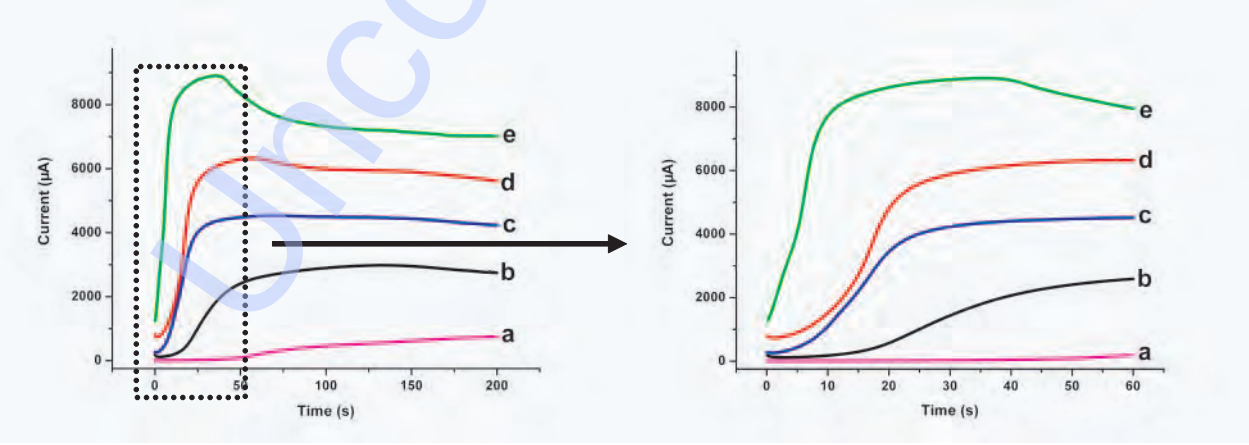

Fig. 1 Chronoamperometric curves of polypyrrole electropolymerization with 30-mer ODN on an ITO electrode surface at different potentials: (a) 0.65 V; (b) 0.7 V; (c) 0.8 V; (d) 0.9 V; (e) 1.0 V

maximum (stage 2, rapid nucleation and growth), and then plateauing out (stage 3, constant nucleation and growth). The first stage is the incubation period, which is characteristic of pyrrole oxidation and oligomer formation [**16**]. When an oligomeric high-density region is formed, the oligomers precipitate upon the electrode surface, thereby resulting in deposition [**17**]. It can be seen from Fig. 1(b) that the incubation period decreases as the electropolymerization potential increases, which is due to the more severe oxidation of polypyrrole at a higher potential [**14**]. In general, the incubation process is rapid, e.g. the incubation period of PPy/ODN is about 10 s at 0.7 V and decreases to about 3 s at 0.9 V. When the applied potential increases to 1.0 V, the process of incubation is too short to be seen.

Figure 2(a) shows chronoamperometric curves of PPy electropolymerization on an ITO electrode surface at 0.8 V during a 200 s period in the presence of three different lengths of ODN and without ODN. It is important to note that the presence of ODN had a significant effect on the nucleation and growth current curves of polypyrrole. Figure 2 (b) shows that the incubation period of polypyrrole electrodeposition in the presence of P1 ODN is about 5 s, while it is prolonged to 30 s without ODN, so it can be presumed that the presence of ODN could greatly shorten the incubation period of polypyrrole electropolymerization. A possible reason for this is that the negatively charged ODN molecule in the polymerization solution was more likely to be electrostatically adsorbed on the positively charged ITO electrode surface as nuclei to initiate a polymerization reaction than the oxidized Py monomer or oligomer with positive charge. Therefore, the mixture of ODN and Py had a shorter incubation period than Py alone. From Fig. 2(b), although there were no distinct differences in incubation period when three different-length ODNs were applied, their different effects remained, e.g. in the presence of 30-mer P1 ODN the incubation time of polypyrrole was about 5 s, which was lightly longer than the 2 s incubation time in the presence of 15-mer P3 ODN. The reason for this might be the stronger affinity of the ODN of shorter length to the electrode, but the precise reason is the subject of intensive research. For a longer polymerization time, a constant current intensity could be observed for PPy/ODN, in contrast to that of pure PPy. This is a further indication that the nucleation and growth mechanism of PPy/ODN is a constant process at this stage. Furthermore, it can be presumed that the negatively charged ODN could be doped in the PPy during polymerization at a constant rate. Moreover, it is also noted that the peak current density of pure PPy is greater than that of PPy/ODN, which can be attributed to the active area of the ITO electrode being reduced by the initial absorption of ODN on the ITO surface.

It is important to study the nucleation and growth mechanism of polypyrrole during electrodeposition. The mechanism of nucleation for conducting polymer growth includes instantaneous and progressive nucleation, and the direction of nucleation includes two-dimensional (2D) and three-dimensional (3D) growth, which is proved by using the theoretic model of metal growth [**18**]. The nucleation and growth mechanism of PPy could be ascertained by comparing the chronoamperometric curves of PPy with the theoretical curves of metallic nucleation and growth [**19**]. A comparative evaluation of experimental data

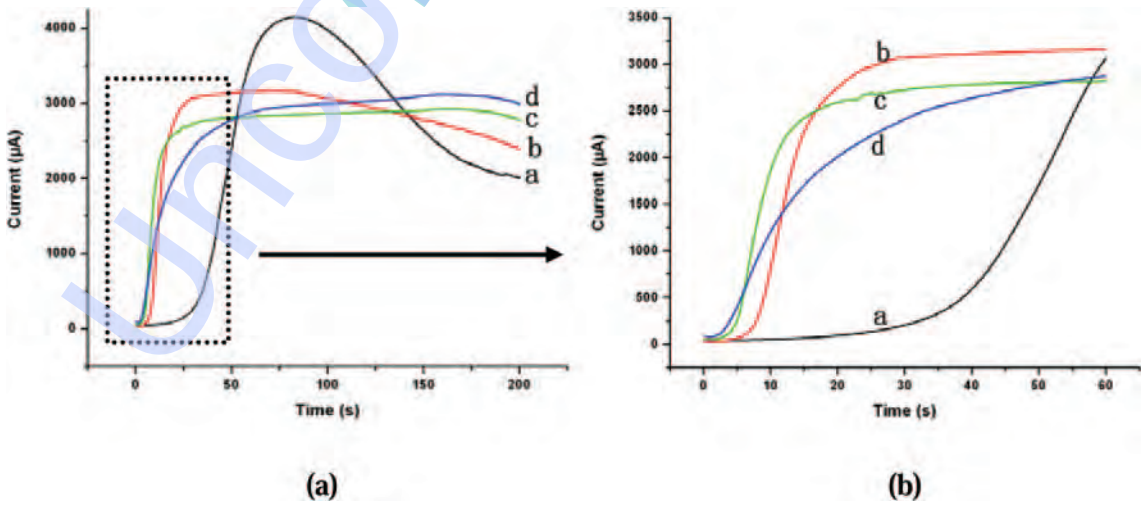

Fig. 2 Chronoamperometric curves of polypyrrole electropolymerization in the presence of different-length ODNs on an ITO electrode surface at 0.8 V: (a) pure PPy; (b) P1 ODN; (c) P2 ODN; (d) P3 ODN

with theoretical curves of progressive/instantaneous nucleation and 2D growth and progressive/instantaneous nucleation and 3D growth is shown in Fig. 3. It is clear that, after nucleus overlapping, the nucleation and growth of PPy/ODN presents a combined mode of progressive and instantaneous nucleation and 3D growth. However, for pure PPy, the third stage is possibly a combination of instantaneous nucleation and 2D growth and progressive nucleation and 3D growth. Before nucleus overlapping, the experimental data for PPy/ODN and PPy deviate considerably from the theoretical curves, so the nucleation and growth mechanism of PPy/ODN cannot be ascertained from this model. However, Fig. 3 indicates the shorter time to reach I_{max} for the PPy/ODN composite than for PPy, which also shows that PPy/ODN has a faster nucleation and growth rate in the first two stages. The reason for this might be that the negatively charged ODN deposited on the electrode surface accelerated the diffusion rate of PPy oligomer towards the electrode interface by electrostatic absorption. On the other hand, the negatively charged ODN and Ppy could be doped directly onto the PPy/ODN composite formed and then become nuclei to initiate a new polymerization, which means that PPy/ODN has a parallel nucleation

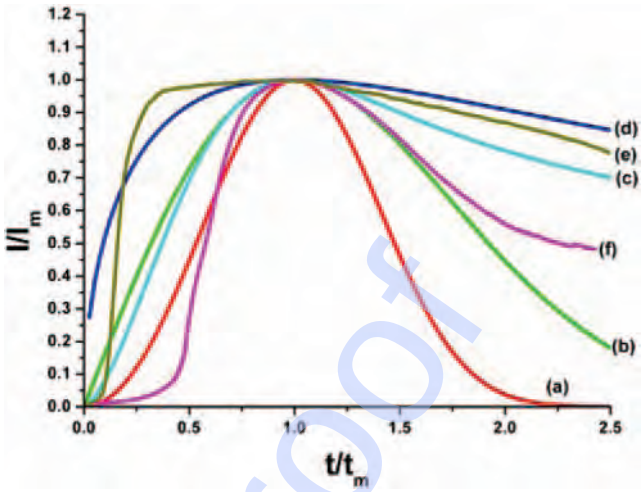

Fig. 3 Dimensionless plots of *I–T* curves (b and d) shown in Fig. 2 for a PPy/ODN nanocomposite (e) and pure PPy (f) compared with the theoretical models for nucleation and growth: (a) progressive nucleation and 2D growth; (b) instantaneous nucleation and 2D growth; (c) progressive nucleation and 3D growth; (d) instantaneous nucleation and 3D growth

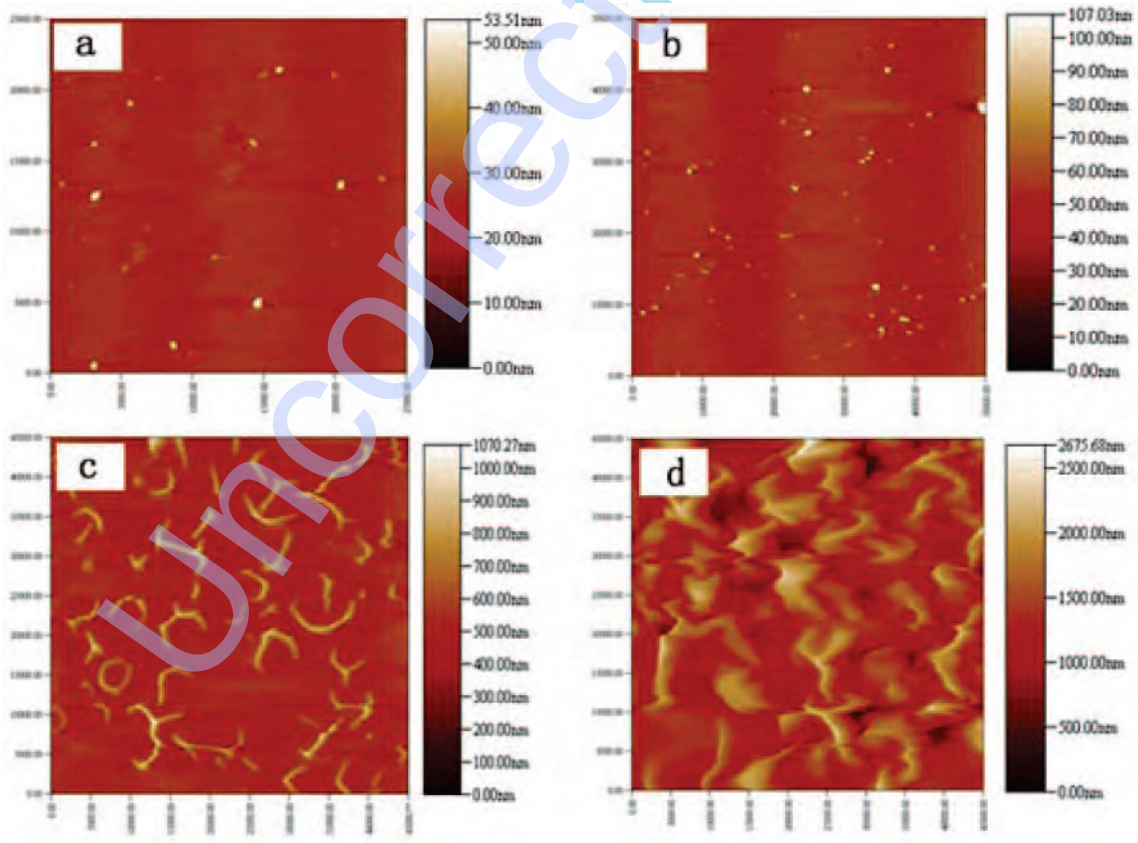

Fig. 4 *Ex situ* AFM images of PPy/ODN prepared at 0.9 V in the presence of P1 ODN for (a) 2 s, (b) 5 s, (c) 20 s, and (d) 60 s

of ODN and Py, while only Py could serve as a nucleus for pure PPy polymerization. This result is similar to that obtained for a polypyrrole/Au nanocomposite [**19**].

3.2 AFM characterization of the PPy/ODN composite

To verify the nucleation and growth mechanism of PPy, AFM has proved to be an effective surface analytical tool [**20**, **21**]. Here, AFM was used to confirm the nucleation and growth mechanism of PPy/ODN before nucleus overlapping. Figure 4 presents *ex situ* AFM micrographs of a PPy/ODN film produced at 0.9 V for different electrodeposition times in the presence of P1 ODN. At the early stage of electrodepositon (a period of 60 s), there is no difference in the AFM micrographs for the three different-length ODNs and different polymerization potentials (0.7, 0.8, and 0.9). After 2 s, some small spots of PPy/ODN appeared on the AFM micrographs (Fig. 4(a)), randomly distributed, with sizes between 5 and 10 nm and maximum heights of 53 nm. However, this is not the case for pure PPy film growth (data not shown). This result indicates that the nucleation of PPy/ODN is faster than that of PPy alone at the incubation stage, which corresponds to the situation presented by the chronoamperometric curves (Fig. 2). Furthermore, Fig. 4(b) indicates that there is a marked increase in the number of PPy/ODN particles after a 5 s electrodeposition time, and their maximum height increases to 107 nm, but their size is the same as in Fig. 4 (a). With a 20–60 s electrodeposition time, the PPy/ODN particles change from Y- or T-shaped units (Fig. 4(c)) and link up with neighbouring PPy/ODN particles to form wrinkles (Fig. 4 (d)). At the same time, the diameters and maximum heights of the PPy/ODN particles increase to 420 nm and 2765 nm respectively. However, the number of PPy/ODN particles is almost constant.

From Figs 4(a) and (b) it can be seen that the size of the PPy/ODN particles increases with electrodeposition time. Meanwhile, it should be noted that the

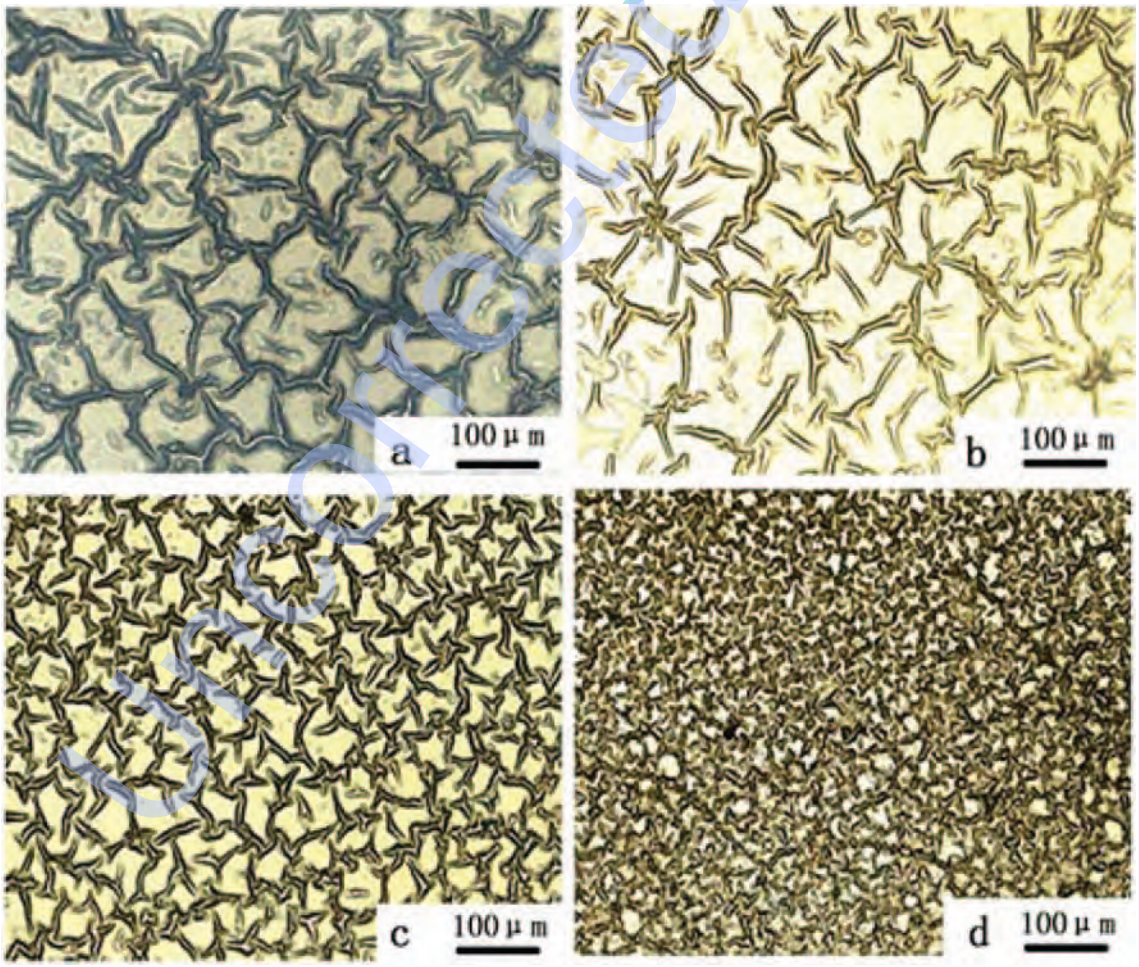

Fig. 5 Optical micrographs of polypyrrole film electropolymerized on an ITO electrode surface at 0.9 V for 200 s in 0.1 M NaCl electrolyte solution with 0.05 M pyrrole and 1×10^{-5} M (a) P1 ODN, (b) P2 ODN, and (c) P3 ODN, and (d) without ODN

height of the surface in the AFM images also increases. Therefore, it can be deduced that the nucleation and growth mechanism of PPy/ODN is mainly progressive nucleation and 3D growth before 5 s. This might be due to the incessant deposition of negatively charged ODN on the electrode surface as new nuclei for initializing new electropolyperization during the first 5 s of deposition. In contrast, in the 20–60 s period, instantaneous nucleation and 3D growth are most prevalent in Figs 3(c) and (d). The reason for such a difference might be that in the former case the negatively charged ODNs are the first species to arrive at the naked ITO surface and act as new nuclei, while in the latter case a number of discrete spots of PPy/ODN have already been formed before the ODNs and Py are adsorbed on the ITO surface, and the ODN and Py are preferentially deposited on the surface of the preformed PPy/ODN rather than on the ITO electrode surface. As a result, these preformed spots of PPy/ODN will gradually increase in size but remain constant in number, and they will then link up with neighbours, finally leading to the formation of wrinkles, as seen in Fig. 4(d).

However, for a longer deposition time, successive AFM image data acquisition was unsuccessful because the height changes occurring during the deposition proved to be too large to handle by the instrument cantilever and fell outside the range of the z-piezotransducer [**22**]. Figure 5 presents optical micrographs of a PPy/ODN film electropolymerized on an ITO electrode surface at 0.9 V for 200 s. It is clear that many wrinkles have formed in the polypyrrole film, which is similar to the results of polypyrrole electrochemical deposition using sodium *p*-toluenesulfonate as dopant in a methanol solution with ITO as the working electrode [**22**]. It has been proved that wrinkle formation in polypyrrole is not an artefact of the handling process of films but is associated with growth on ITO substrates [**22**, **23**]. It is important to note that the size of the wrinkles in PPy/ODN after 200 s electrodeposition (Figs 5(a) to (c)) was greater than that for PPy alone (Fig. 5(d)), and a shorter ODN length resulted in a smaller wrinkle size. Therefore, ODN, as a chain-like, negatively charged molecule, could be used as a template to guide the synthesis of PPy/ODN composites at least during the initial electropolymerization process.

4 CONCLUSION

In summary, the initial electrochemical growth of a PPy/ODN nanocomposite on an ITO-coated glass surface has been investigated. It was found that ODN with a negative charge can be deposited onto the ITO electrode and preformed PPy/ODN surface to serve as nuclei for a new polypyrrole electrodeposition process. The nucleation and growth mechanism of PPy/ODN was found to be progressive nucleation and 3D growth in the first 5 s, which then changed to instantaneous nucleation and 3D growth before nucleus overlapping. However, the nucleation and growth mechanism of PPy/ODN was found to be a combination of progressive nucleation and 3D growth and instantaneous nucleation and 3D growth after nucleus overlapping. Additionally, optical microscopy and AFM images show a clear morphology of wrinkles in the PPy/ODN film. As a chain-like, negatively charged molecule, ODN could serve as a template to guide the electropolymerization of PPy. These results may provide fundamental insights into the nucleation and growth mechanism of polypyrrole in the presence of chain-like biomolecules, which might be further applied in areas such as genoelectronic devices, bioactive interfaces, or probing DNA charge transfer.

ACKNOWLEDGEMENTS

This paper was supported by the Key Project for International Science and Technology Collaboration of the Ministry of Science and Technology (2005DFA00190) and by an NSFC grant (30870607), a CSTC grant (2008BB5192), and the '111 Project' (B06023).

REFERENCES

1 **Yoshihiro, I.** and **Eiichiro, F.** DNA as a 'nanomaterial'. *J. Molec. Catalysis B: Enzymatic*, 2004, **28**(4–6), 155–166.
2 **Dong, L., Hollis, T., Fishwick, S., Connolly, B. A., Wright, N. G., Horrocks, B. R.,** and **Houlton, A.**. Synthesis, manipulation and conductivity of supramolecular polymer nanowires. *Chem. Eur. J.*, 2007, **13**(3), 822–828.
3 **Stela, P., Farha Al-Said, S. A., Dong, L., Hollis, T. A., Galindo, M. A., Wright, N. G., Houlton, A.,** and **Horrocks, B. R.** Self-assembly of DNA-templated polypyrrole nanowires: spontaneous formation of conductive nanoropes. *Adv. Funct. Mater.*, 2008, **18**(16), 2444–2454.
4 **Mandala, S. K.** and **Dutta, P.** Synthesis of DNA–polypyrrole nanocapsule. *J. Nanosci. and Nanotechnol.*, 2004, **4**(8), 972–975.
5 **Peng, H., Zhang, L. J., Soeller, C.,** and **Jadranka, T. S.** Conducting polymers for electrochemical DNA sensing. *Biomaterials*, 2009, **30**, 2132–2148.
6 **Drummon, T. G., Michael, G. H.,** and **Barton, J. K.** Electrochemical DNA sensors. *Nature Biotechnol.*, 2003, **21**, 1192–1199.

7 **Serge, C.** Affinity biosensors based on electropolymerized films. *Electroanalysis*, 2005, **17**(19), 1701–1715.

8 **Joseph, W.** and **Mian, J.** Toward genoelectronics: nucleic acid doped conducting polymers. *Langmuir*, 2000, **16**(5), 2269–2274.

9 **Tosar, J. P., Karen, K.,** and **Laíz, J.** Two independent label-free detection methods in one electrochemical DNA sensor. *Biosensors and Bioelectronics*, 2009, DOI:10.1016/j.bios.2009.03.016.

10 **Peng, H., Soeller, C., Mark, B. C., Graham, A. B., Ralph, P. C.,** and **Jadranka, T. S.** Electrochemical detection of DNA hybridization amplified by nanoparticles. *Biosensors and Bioelectronics*, 2006, **21**(9), 1727–1736.

11 **Qi, H., Li, X., Chen, P.,** and **Zhang, C.** Electrochemical detection of DNA hybridization based on polypyrrole/ss-DNA/multi-wall carbon nanotubes paste electrode. *Talanta*, 2007, **72**(3), 1030–1035.

12 **Martins, N. C. T., Silva, T. M., Montemor, M. F., Fernandes, J. C. S.,** and **Ferreira, M. G. S.** Electrodeposition and characterization of polypyrrole films on aluminium alloy 6061-T6. *Electrochim. Acta*, 2008, **53**(14), 4754–4763.

13 **Hwang, B. J., Raman, S.,** and **Lin, Y. L.** Evaluation of structure, nucleation and growth mechanism of electropolymerized polypyrrole on highly oriented pyrolytic graphite electrode. *Electroanalysis*, 2003, **15**(2), 115–120.

14 **Yan, W.** and **Derek, O. N.** An investigation into the nucleation and growth of an electropolymerized polypyrrole coating on a 316L stainless steel surface. *Thin Solid Films*, 2008, **516**(21), 7427–7432.

15 **Wang, B. J., Santhanam, R.,** and **Lin, Y. L.** Nucleation and growth mechanism of electroformation of polypyrrole on a heat-treated gold/highly oriented pyrolytic graphite. *Electrochim. Acta*, 2001, **46**(18), 2843–2853.

16 **Cossement, D., Plumier, F., Delhalle, J., Hevesi, L.,** and **Mekhalif, Z.** Electrochemical deposition of polypyrrole films on organosilane-modified ITO substrates. *Synthetic Metals*, 2003, **138**(3), 529–536.

17 **Valle, M. A., Cury, P.,** and **Schrebler, R.** Solvent effect on the nucleation and growth mechanisms of poly (thiophene). *Electrochim. Acta*, 2002, **48**(4), 397–405.

18 **Sarkar, D. K., Zhou, X. J., Tannous, A.,** and **Leung, K. T.** Growth mechanisms of copper nanocrystals on thin polypyrrole films by electrochemistry. *J. Phys. Chem. B*, 2003, **107**, 2879–2881.

19 **Chen, W., Li, C. M., Yua, L., Lua, Z.,** and **Zhoua, Q.** In situ AFM study of electrochemical synthesis of polypyrrole/Au nanocomposite. *Electrochem. Commun.*, 2008, **10**(9), 1340–1343.

20 **Chen, W., Li, C. M., Chen, P.,** and **Sun, C. Q.** Electrosynthesis and characterization of polypyrrole/Au nanocomposite. *Electrochim. Acta*, 2007, **52**(8), 2845–2849.

21 **ElKaoutit, M., Naggar, A. H., Ignacio, N. R., Dominguezc, M.,** and **JoséLuis, H. H. C.** Electrochemical AFM investigation of horseradish peroxidase enzyme electro-immobilization with polypyrrole conducting polymer. *Synthetic Metals*, 2009, **159**(5–6), 541–545.

22 **Miles, M. J., Smith, W. T.,** and **Shapiro, J. S.** Morphological investigation by atomic force microscopy and light microscopy of electropolymerised polypyrrole films. *Polymer*, 2000, **41**(9), 3349–3356.

23 **Shapiro, J. S.** and **Smith, W. T.** A morphological study of polypyrrole films grown on indium-tin oxide conductive glass. *Polymer*, 1997, **38**(22), 5505–5514.